EBEX: the E and B Experiment

Will Grainger, Asad M. Aboobaker, Peter Ade, François Aubin, Carlo Baccigalupi, et al.

Will Grainger, Asad M. Aboobaker, Peter Ade, François Aubin, Carlo Baccigalupi, Éric Bissonnette, Julian Borrill, Matt Dobbs, Shaul Hanany, Clayton Hogen-Chin, Johannes Hubmayr, Andrew Jaffe, Bradley Johnson, Terry Jones, Jeff Klein, Andrei Korotkov, Sam Leach, Adrian Lee, Lorne Levinson, Michele Limon, John Macaluso, Kevin MacDermid, Tomotake Matsumura, Xiaofan Meng, Amber Miller, Michael Milligan, Enzo Pascale, Dan Polsgrove, Nicolas Ponthieu, Britt Reichborn-Kjennerud, Tom Renbarger, Ilan Sagiv, Federico Stivoli, Radek Stompor, Huan Tran, Greg Tucker, Jerry Vinokurov, Matias Zaldarriaga, Kyle Zilic, "EBEX: the E and B Experiment," Proc. SPIE 7020, Millimeter and Submillimeter Detectors and Instrumentation for Astronomy IV, 70202N (21 July 2008); doi: 10.1117/12.789627

SPIE.

Event: SPIE Astronomical Telescopes + Instrumentation, 2008, Marseille, France

EBEX - The E and B Experiment

Will Grainger[a], Asad M. Aboobaker[b], Peter Ade[c], François Aubin[d], Carlo Baccigalupi[e], Eric Bissonnette[d], Julian Borrill[f,g], Matt Dobbs[d], Shaul Hanany[b], Clayton Hogen-Chin[b], Johannes Hubmayr[b], Andrew Jaffe[h], Bradley Johnson[i], Terry Jones[b], Jeff Klein[b], Andrei Korotkov[j], Sam Leach[e], Adrian Lee[k], Lorne Levinson[l], Michele Limon[a], John Macaluso[j], Kevin MacDermid[d], Tomotake Matsumura[m], Xiaofan Meng[k], Amber Miller[a], Michael Milligan[b], Enzo Pascale[c], Dan Polsgrove[b], Nicolas Ponthieu[n], Britt Reichborn-Kjennerud[a], Tom Renbarger[o], Ilan Sagiv[b], Federico Stivoli[e], Radek Stompor[p], Huan Tran[g], Greg Tucker[j], Jerry Vinokurov[j], Matias Zaldarriaga[q] and Kyle Zilic[b]

[a]Columbia University, New York, NY 10027,
[b]University of Minnesota School of Physics and Astronomy, Minneapolis, MN 55455,
[c]Cardiff University, Cardiff, CF24 3AA, United Kingdom,
[d]McGill University, Montréal, Quebec, H3A 2T8, Canada,
[e]Scuola Internazionale Superiore di Studi Avanzati, Trieste 34014, Italy,
[f]National Energy Research Supercomputing Center, Lawrence Berkeley National Laboratory,
[g]University of California, Berkeley, Space Sciences Lab, Berkeley, CA 94720,
[h]Imperial College, London, United Kingdom,
[i]Oxford University, Oxford, OX1 3RH, England, United Kingdom,
[j]Brown University, Providence, RI 02912,
[k]University of California, Berkeley, Berkeley, CA 94720,
[l]Weizmann Institute of Science, Rehovot 76100, Israel,
[m]California Institute of Technology, Pasadena, CA 91125,
[n]Institut d'Astrophysique Spatiale, Universite Paris-Sud, Orsay, 91405, France,
[o]University of California, San Diego,
[p]Laboratoire Astroparticule et Cosmologie (APC), Université Paris Diderot, Paris Cedex 13, 75205, France,
[q]Harvard University Center for Astrophysics, Cambridge, MA 02138.

ABSTRACT

The E and B Experiment, *EBEX*, is a Cosmic Microwave Background polarization experiment designed to detect or set upper limits on the signature of primordial gravity waves. Primordial gravity waves are predicted to be produced by inflation, and a measurement of the power spectrum of these gravity waves is a measurement of the energy scale of inflation. *EBEX* has sufficient sensitivity to detect or set an upper limit at 95% confidence on the energy scale of inflation of $< 1.4 \times 10^{16}$ GeV. This article reviews our strategy for achieving our science goals and discusses the implementation of the instrument.

1. INTRODUCTION

The paradigm of inflation,[1–4] in which the Universe underwent exponential expansion within its first $\sim 10^{-35}$ sec, is consistent with all current astrophysical measurements.[6,21] It is the leading model of the state of the Universe at early times that convincingly explains puzzling cosmological phenomena.[7] However, many of the details of the inflationary scenario are uncertain, and the paradigm currently lacks any strong confirmation. Inflation predicts a stochastic background of gravity waves, the inflationary gravity wave background (IGB).[8–12] The amplitude of

Further author information: Send correspondence to W.F.G. E-mail: grainger@astro.columbia.edu

Millimeter and Submillimeter Detectors and Instrumentation for Astronomy IV
edited by William D. Duncan, Wayne S. Holland, Stafford Withington, Jonas Zmuidzinas
Proc. of SPIE Vol. 7020, 70202N, (2008) · 0277-786X/08/$18 · doi: 10.1117/12.789627

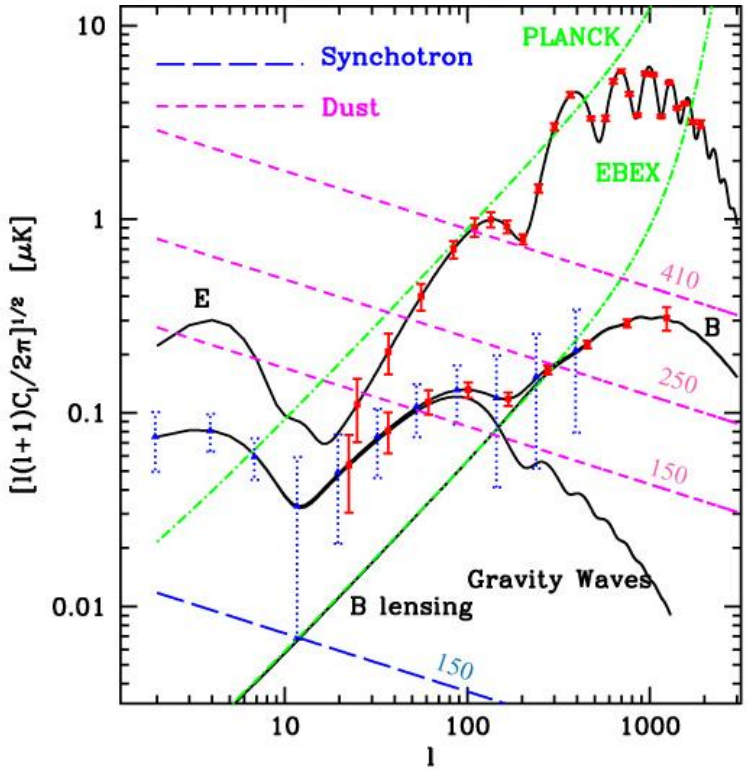

Figure 1. The power spectra for B and E-modes for a T/S = 0.1 ΛCDM universe (black lines), with predicted instrumental noise and cosmic variance error bars for *EBEX* (red) and Planck 1 year (blue). The upper black line, labeled 'E', is the E-mode, and 'B' is the B-mode signal, which comes from both the lensing signal and IGB (labeled 'Gravity waves'). Also shown is a model of expected dust and synchrotron signal levels in our frequency bands and within the LD sky patch. Finally, the power spectra of pixel noise (green) are shown for both Planck and EBEX.

the IGB is predicted to be proportional to the energy scale of inflation, $V^{1/4}$, via $V^{1/4} = 3.7 \times 10^{16} (T/S)^{1/4}$ GeV, where $T/S = C_2^{GW}/C_2^S$ is the ratio of the temperature quadrupoles produced by gravity waves and by density perturbations, and V is the inflaton potential. The current 2σ upper limit[5] of $T/S \approx 0.2$ implies $V^{1/4} < 2.5 \times 10^{16}$ GeV.

The best known way to search for the IGB is through its signature on the Cosmic Microwave Background (CMB) polarization.[13,14] Primordial energy density perturbations produce a curl-free ('E-mode') polarization pattern. The IGB produces both an E-mode and a curl ('B-mode') pattern of polarization vectors that density perturbations alone cannot produce.[15,16] The amplitude of the B-mode signal is related to the energy scale of inflation by $V^{1/4} = 2 \times 10^{16} (B_{\rm peak}/0.1\mu{\rm K})^{1/2}$ GeV where $B_{\rm peak}$ is the amplitude of the power spectrum of the B-mode in μK at $l = 90$.

The E and B Experiment (*EBEX*) is a balloon borne CMB polarization experiment designed to observe the E and B-mode polarization. It is due for a test launch from Fort Sumner, New Mexico in September 2008, and a long duration (LD) balloon flight in the 2010 from McMurdo base, Antarctica. In this paper we will outline our science goals and discuss the experimental details of how this measurement will be performed.

2. SCIENCE GOALS

EBEX has a number of science goals, which we will enumerate while referencing Figure 1.

Detect or set an upper limit on the IGB signal. The lower curve of Figure 1, labeled Gravity Waves, shows the IGB power spectrum of the CMB in a standard ΛCDM cosmology for a tensor to scalar ratio $T/S = 0.1$. The red error bars show the expected 1σ determination of the overall B-mode for a 14 day *EBEX* LD flight. If

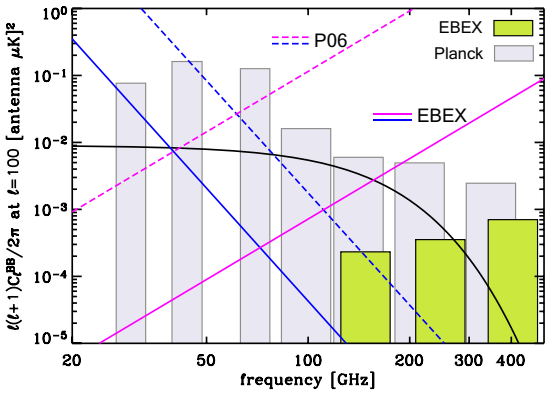

Figure 2. Spectrum of B-mode foregrounds from Galactic dust (magenta) and synchrotron (blue) expected outside of WMAP's P06 mask[27] (dashed) and our estimate in the *EBEX* area (solid), and the B-mode CMB (black), all at $l = 100$. The *EBEX* (green histograms) and Planck noise (light gray histograms) levels in their respective frequency bands are also shown.

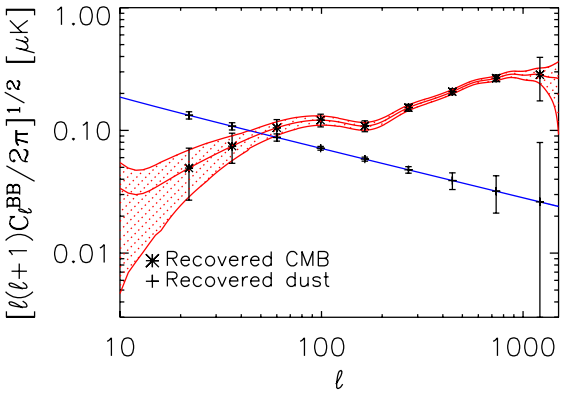

Figure 3. B-mode signal reconstruction with dust correction. dust subtraction. The input CMB B-mode power spectrum (solid red), and calculated power spectrum of the simulated dust map (solid blue) are shown. The results of 10 map domain simulations (that include instrumental noise) of the reconstruction of the CMB (black crosses) and dust (black squares) are shown with errors. The overall increase in the errors over the majority of the l range is small.

the T/S ratio is close to 0.1, *EBEX* will detect the IGB signal and thus determine the energy scale of inflation. If the B-mode signal is not detected, we will put a 2σ upper limit on $T/S < 0.02$, corresponding to an energy scale of 1.4×10^{16} GeV. This would rule out so-called 'classic inflationary' models, often considered the simplest models of inflation.[18]

Measure the B-mode CMB lensing signal. Gravitational lensing of CMB photons along the line of sight by large-scale structures in the Universe distorts the E-mode polarization, modifies its power spectrum[19] and creates a B-mode polarization even if gravity waves are not present.[20] The curve labeled 'B' on Figure 1 shows the combined B-mode spectrum from both the IGB and lensing, and the curve 'B lensing' shows the lensing alone. Currently the amplitude of the lensing B-mode signal is predicted to within $\approx 20\%$[21,22] (from existing large scale structure and E-mode measurements). *EBEX* is designed to detect and constrain the amplitude of this component with an accuracy of $\approx 7\%$.

Characterize the polarized dust emission in both E and B-mode polarizations. CMB measurements have three primary sources of contaminating foreground emission: dust, synchrotron, and extra-galactic point-sources. A plot of the dust and synchrotron power spectra is shown in Figure 2. In the low foreground area selected for the LD flight, synchrotron is expected to be sub-dominant at 150 GHz and even less significant at higher frequencies. However, the signal level from dust is expected to be comparable to the cosmological signal at 150 GHz, and larger at higher frequencies. With three frequencies centered on 150, 250 and 410 GHz, and 752, 376 and 278 detectors in those bands, respectively, simulations show that *EBEX* should have the sensitivity to subtract the dust foreground and reconstruct the power spectrum of the B-mode, with only a small increase in uncertainty; see Figure 3. To calculate the results in this Figure we produced ten realizations of CMB B-mode, dust signal and instrument noise. Using a parametric approach[26] we estimated both the dust and CMB signal and assessed the additional error on the reconstruction of the CMB signal coming from this simultaneous estimate. We find that for $\ell < 900$ the increase in error is less than 30% compared to the error coming from instrument noise and sample variance.

Make a cosmic-variance limited measurement of the E-mode CMB power spectrum. *EBEX* will make cosmic variance limited measurements of the E-mode spectrum from $25 < l < 1500$. These measurements will improve the accuracy of determination of cosmological parameters.

The experimental design is driven to meet these science goals. An important challenge is to control systematics sufficiently to allow the measurement of the faint B-mode in the presence of brighter E-modes and foreground

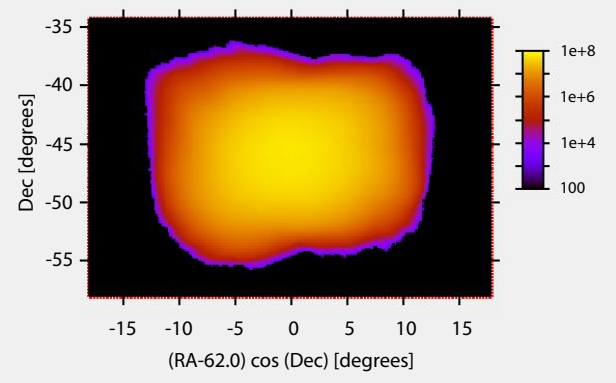

Figure 4. Detector sample counts for *EBEX* in our LD sky patch. The count is for the 752 150 GHz detectors and a 14 day flight.

contaminants.

3. SCAN STRATEGY

The range of angular scales we have chosen to probe sets both the resolution (and hence beam size of the instrument) and the size of the sky patch we scan. Figure 1 shows the expected measurement achievable with a 14 day flight (the average for LD[17]) and 752 150 GHz detectors if we observe 350 square degrees of sky. The scan strategy is to perform a sawtooth scan in azimuth stepping in elevation after 4 scans. Scanning in azimuth ensures uniform atmospheric loading. The scan speed is 0.7 sec, and the amplitude of the sawtooth is 17 degrees. After the elevation has changed by 10 degrees in declination the sequence is restarted. This scan strategy provides re-visitation of pixels on multiple timescales and with different orientation between the instrument and fixed coordinates on the sky (i.e. cross-linking). Both of these are important for minimizing instrumental systematics. The sky coverage achieved is shown in Figure 4.

4. EXPERIMENTAL IMPLEMENTATION

The experimental platform is shown in Figure 5. In order to make broad-band observations between 150 and 410 GHz, the telescope must be above the atmosphere, so *EBEX* is designed to fly on a high-altitude balloon. In this section we discuss the subsystems.

4.1 Balloon platform and control

The overall gondola design is shown in figure 5. The inner frame holds the optics, cryostat, readout and power crates, gyroscopes and star cameras. The outer frame holds the attitude control system readout and power systems, flight computer, reaction wheel, and Columbia Scientific Balloon Facility's flight support electronics. The azimuth attitude is controlled by controlling the acceleration of the reaction wheel, and a motor in the rotator allows torque to be applied against the flight-line to prevent the reaction wheel from saturating. The elevation between inner and outer frame is measured with a 16 bit encoder, and controlled with a linear actuator.

The highest accuracy absolute pointing determination is provided with star cameras taking images at the stationary points of each scan. In order to track the gondola's motion between these points, three fiber-optic rate gyroscopes provide continuous angular velocity information around three orthogonal axes. This data stream is then integrated to provide pointing reconstruction to better than 10 arc-sec at all points along the scan.

A number of additional pointing systems provide redundancy for attitude determination and control. A two-axes magnetometer, sun sensor and differential GPS system all provide coarse real time attitude information. The flight computer determines the real time RA and Dec from an average of the sensors weighted by their measured noise. In addition, the flight computer also controls the rest of the subsystems, runs the observing schedule and writes all data to disk. The system is designed to run autonomously for the flight.

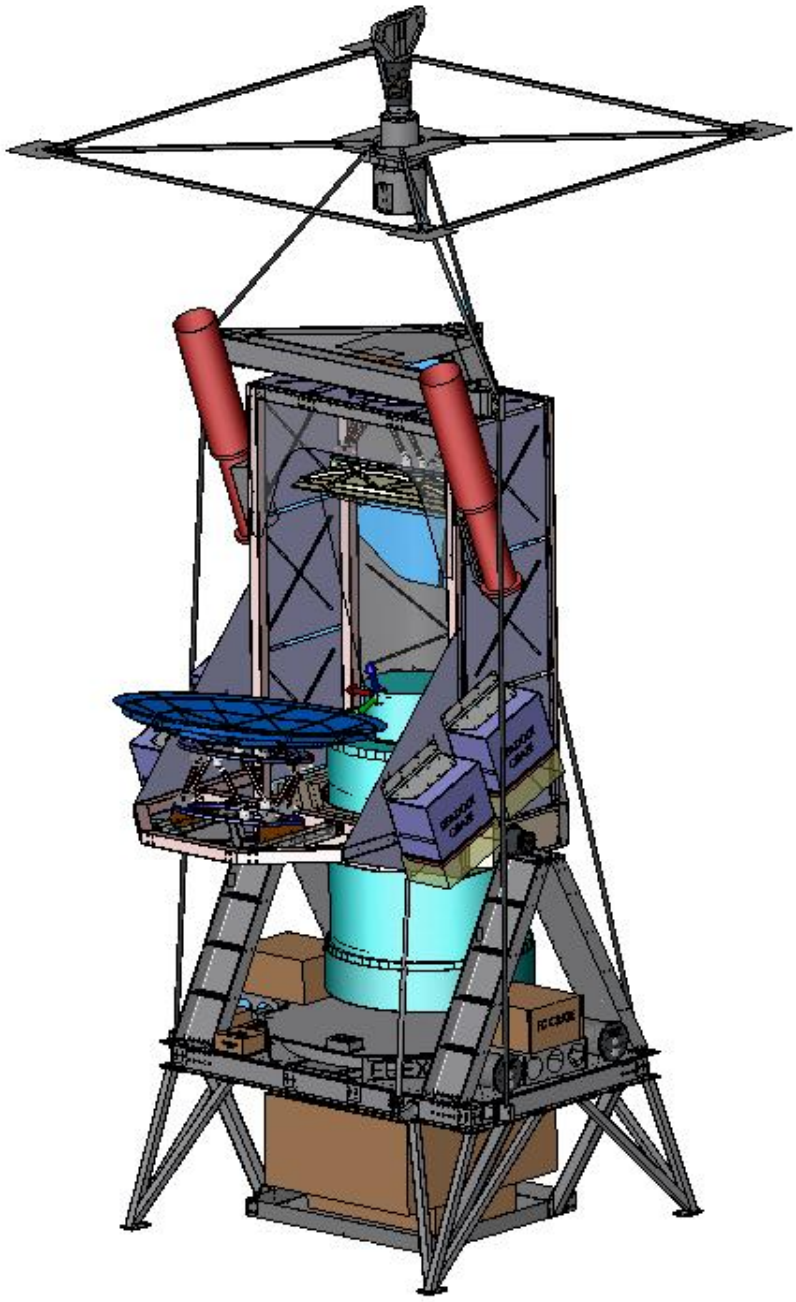

Figure 5. *EBEX* Gondola without sun shields or solar cells.

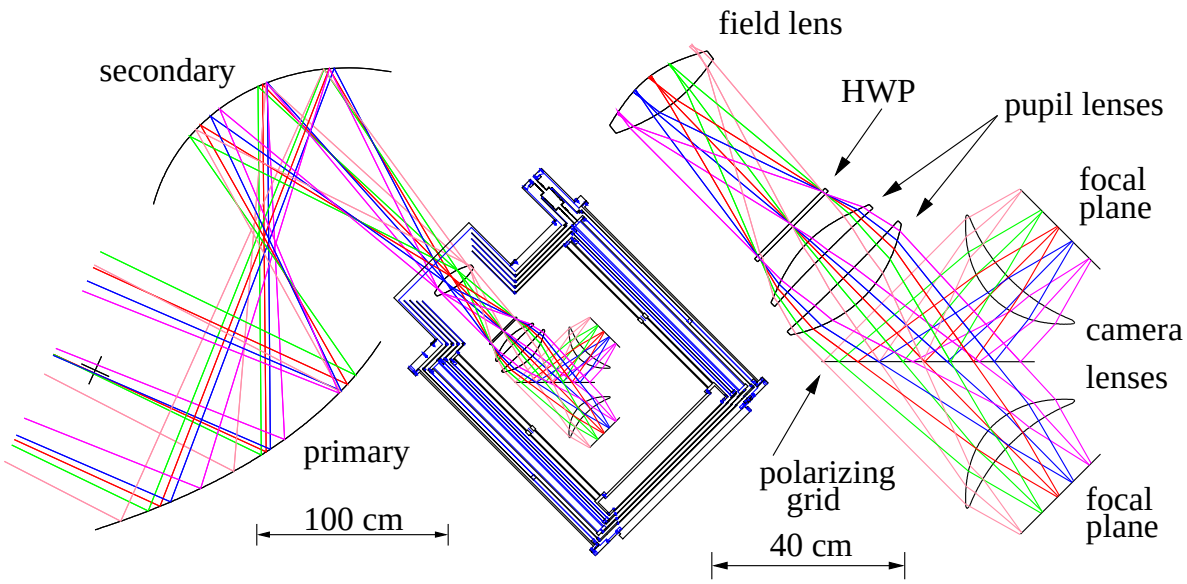

Figure 6. *EBEX* Optical system.

4.2 Optics

The *EBEX* optical design was driven by a number of criteria. The focal plane must be flat as the detectors are manufactured together on wafers. The aperture should be unobstructed to reduce reflections that could increase the instrumental polarization (IP). There should be a cold Lyot-stop to reduce the side-lobe level. The field of view should be large and diffraction limited to increase mapping speed. Finally, the entire system should be compact.

The *EBEX* optical design, shown in Figure 6, consists two reflectors in a Gregorian Mizuguchi-Dragone configuration, coupled to cold re-imaging optics. The primary is the 1.5 m *Archeops*[23] primary. A new secondary with semi-major and semi-minor axes of 1.10 and 0.98 m respectively provides an effective focal length of -198 cm and couples the light to the cold optics inside the cryostat.

The five cold re-imaging lenses provide a flat telecentric focal plane. The cold Lyot-stop is between the field lens and the first pupil lens. The HWP, discussed in Section 4.5 is located at the Lyot-stop. A 42 cm diameter polarizing grid, oriented at 45 degrees to the incident radiation acts both as a polarization analyzer and a beam splitter, passing one orientation of the polarization to one focal plane, and reflecting the other into a second focal plane. Modulating the polarization with a HWP gives strong rejection of polarimetric systematic errors. The mirrors, receiver window, thermal filters and one re-imaging lens are the only optical components on the sky side of the HWP. Special attention is paid to these components to mitigate potential systematic errors. The mirrors are expected to induce 0.1% IP. The window and lens are made from Ultra-High Molecular Weight Polyethylene, with a broad-band anti-reflection (AR) coating. By using a second "weather" window at ground level that is removed at float, the window will be flat at float pressure, eliminating a large source of potential IP due to reflections from the tilted surfaces. It is expected that IP from the window, field lens and filter will be around 0.1%.

The lenses couple the optical radiation into a hexagonal array of smooth-walled conical feed horns. The horns for different frequencies have the same physical diameter, giving the higher frequencies a narrower beam at the focal plane. The Lyot-stop truncates the beam at 4K. Thus the aperture illumination at the primary is a Gaussian truncated with a top-hat, resulting in the far-field beam-widths given in Table 1.

4.3 Cryostat

The cryostat, which holds the cold optics at 4 K and the detectors at less than 300 mK, contains a liquid helium bath held at atmospheric pressure, surrounded by a liquid nitrogen bath and vapor-cooled shields. The cryostat

Frequency	$\mathrm{FWHM_{sky}}$	Edge taper at aperture stop
150 GHz	7.76'	-7.2 dB
250 GHz	5.82'	-19.4 dB
410 GHz	5.02'	-50 dB

Table 1. *EBEX* optical parameters

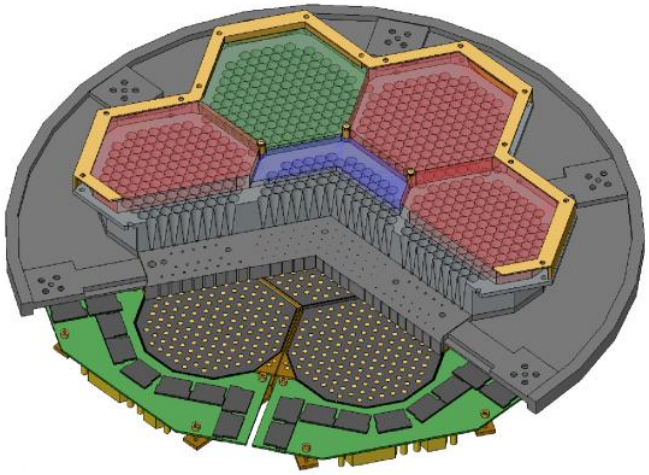

Figure 7. *EBEX* focal plane. The hexagons in red are the 150 GHz filters, in green are the 250 GHz filters and the central blue hexagon is the 410 GHz filter. The TES wafers below the conical smooth-bore horns are shown in gray and yellow.

is designed for a hold time of 21 days. The detectors are cooled using a ^{3}He adsorption refrigerator.

4.4 Detectors

The detectors for *EBEX* are transition edge sensor (TES) bolometers. Each wafer, which is a decagon, is a hexagonal array of 139 bolometers and each focal plane is then made up of 7 decagons. The expected noise equivalent power (NEP) of a single bolometer is 3.8×10^{-17} W/$\sqrt{\mathrm{Hz}}$. This is the quadrature sum of the (dominant) phonon noise and TES Johnson noise. Figure 7 shows a cut-away diagram of one of the focal planes.

Detector readout is performed by a new low-power digital frequency multiplexing scheme.[24,25] The readout noise of the system (i.e. the SQUID and electronics) is measured as 1.9×10^{-18} W/$\sqrt{\mathrm{Hz}}$, lower than the expected noise from the bolometer. The power draw for the LD flight is estimated at 550 W.

4.5 Half wave plate

Polarimetry is performed with an achromatic half wave plate (HWP) continuously rotated at 6 Hz in the Lyot-stop of the cold optics. The achromatic half wave plate is made by stacking 5 chromatic sapphire HWPs, each 1.62 mm thick, at orientations of (0, 25, 85, 25, 0)° relative to the crystal axis of the first. The HWP is AR coated with expanded Teflon. Figure 8 shows the modulation efficiency of this stack. The HWP is driven continuously via a Kevlar belt and is supported by a superconducting magnetic bearing operating at 4 K.[28] Superconducting bearings are suitable for this application because they can have friction that are smaller than the friction of standard bearings by a factor of up to 10,000, decreasing heat load and increasing cryogen hold time.

5. CONCLUSION

We have discussed the design of *EBEX*, a balloon-borne CMB polarization experiment. *EBEX* is designed to constrain the amplitude of B-modes in a cosmologically interesting range, probing the earliest moments of the universe. In addition, *EBEX* should provide E-mode measurements, B-mode lensing measurements and information about polarized foregrounds in the frequency range 150 to 410 GHz.

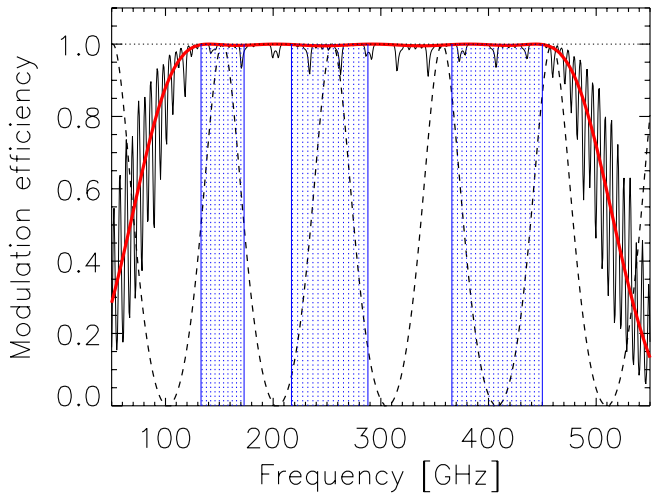

Figure 8. EBEX HWP predicted modulation efficiency as a function of frequency (with reflections: oscillatory black curve, without reflection between plates: red), compared to a chromatic HWP (black, dashed).

Acknowledgments

EBEX is a NASA supported mission through grant number NNX08AG40G. We also acknowledge support from the Canadian Institute for Advanced Research, CNRS, Minnesota Supercomputing Institute, NSF GK-12 grant 0638688, Rhode Island Space Grant, and the Science and Technology Facilities Council. This research used resources of the National Energy Research Scientific Computing Center, which is supported by the Office of Science of the U.S. Department of Energy under Contract No. DE-AC02-05CH11231. CB was supported in part by the NASA LTSA Grant NNG04CG90G, and BJ acknowledges a PPARC Postdoctoral Fellowship and NSF IRFP Fellowship.

REFERENCES

[1] A.H. Guth, *Phys. Rev.* D **23**, 347 (1981).
[2] A.D. Linde, *Phys. Lett.* B **108**, 389 (1982).
[3] A. Albrecht and P. J. Steinhardt, *Phys. Rev. Lett.* **48**, 1220 (1982).
[4] K. Sato, MNRAS **195**, 467 (1981).
[5] E. Komatsu, *et al*, astro-ph 0803.0547.
[6] M. Tegmark *et al*, *Phys. Rev.* D **74**, 123507 (2006).
[7] E.W. Kolb and M.S. Turner in *The Early Universe*, (Addison-Wesley, CA, 1994).
[8] A.A. Starobinsky, *Phys. Lett.* B **117**, 175 (1982).
[9] A. A. Starobinskii, Soviet Astro Lett **9**, 302 (1983).
[10] V.A. Rubakov *et al*, *Phys. Lett.* B **115**, 189 (1982).
[11] L.P. Grishchuk, Sov Phys. JETP **40**, 409 (1975).
[12] L. F. Abbott and M. B. Wise, Nuclear Physics B **244**, 541 (1984).
[13] M.Kamionkowski *et al*, *Phys. Rev.* D **55**, 7368 (1997).
[14] U. Seljak and M. Zaldarriaga, *Phys. Rev. Lett.* **78**, 2054 (1997).
[15] M.Kamionkowski *et al*, *Phys. Rev. Lett.* **78**, 2058 (1997).
[16] M.Zaldarriaga and U.Seljak., *Phys. Rev.* D **55**, 1830 (1997).
[17] D. Ball (CSBF Head of Operations), 2004. Private communication.
[18] J.Bock *et al*, Task force on cosmic microwave background research, 2006.
[19] U.Seljak, ApJ **482**, 6 (1997)

[20] M.Zaldarriaga and U.Seljak, *Phys. Rev.* D **58**, 23003 (1998).
[21] E. Komatsu, *et al*, astro-ph 0803.0547v1.
[22] M.Tegmark, *el al*, *Phys. Rev.* D **69**, 103501 (2004).
[23] A.Benoit, *et al*, Astropart. Phys **17**, 101 (2002).
[24] M.Dobbs, *et al*, *Proc SPIE NPSS Real Time Conf.*
[25] J.Hubmayr, *et al*, *Proc SPIE Astro.Inst.*
[26] R.Stompor, *et al* astro-ph 0804.2645 , (2008)
[27] L.Page, *et al* ApJS **170**, 335 (2007)
[28] S.Hanany, *et al* IEEE Applied Superconductivity **13**, 2128 (2003).